

Optimal Design of a Geothermal Organic Rankine Cycle System

Jui-Yuan Lee*, Shan-Long Chen

Department of Chemical Engineering and Biotechnology, National Taipei University of Technology, 1, Sec 3, Zhongxiao E Rd, Taipei 10608, Taiwan, ROC
 juiyuan@ntut.edu.tw

Compared with conventional Rankine cycles that use water as the working fluid, organic Rankine cycles (ORCs) can produce shaft work/power from low-to-medium temperature heat sources more efficiently. Other advantages of ORCs include long service life, low maintenance cost and improved part-load characteristics. ORCs have been applied to power generation from different heat sources such as industrial waste heat, solar thermal, biomass and geothermal. This work focuses on the application of ORCs for geothermal power generation, considering different possible ORC configurations. A generic design method involving thermodynamic analysis and process modelling is developed, with the aim of assessing the system performance as well as determining the optimal system configuration and operating conditions. A literature case study is presented to illustrate the proposed approach.

1. Introduction

Renewables (i.e. bioenergy, wind, solar, hydroelectricity and geothermal) play a central role in the global pathway to net-zero emissions by 2050, expected to provide two thirds of energy use in 2050, according to a recent report of the International Energy Agency (IEA, 2021). Geothermal is one of the main dispatchable renewables globally in 2050, producing low-temperature heat for use in industries. When geothermal is used for electricity generation, the thermal efficiency is an issue.

The organic Rankine cycle (ORC) uses an organic working fluid of which the boiling point is lower than water, and is able to produce power from low-to-medium temperature heat sources more efficiently than a conventional Rankine cycle. Other advantages of ORCs over conventional Rankine cycles include long service life, low maintenance cost and improved part-load characteristics. ORCs have been applied to power generation from various sources such as industrial waste heat, biomass, solar thermal and geothermal.

There have been a few works on the design of geothermal ORC systems using mathematical programming approaches. Elsidio et al. (2017) presented a superstructure-based method for the optimisation of integrated ORC and heat exchanger network (HEN) systems, considering a range of cycle configurations. Their method was applied to a case study of a typical binary geothermal power plant. Tien et al. (2020) addressed the design of ORC-based geothermal binary power systems under economic and environmental criteria, and formulated a superstructure-based life cycle optimisation model to determine the optimal design. Their model was applied to two case studies of geothermal energy systems in California and New York State. Dong et al. (2020) proposed a simultaneous optimisation model to determine the optimal ORC operating conditions and HEN structure, considering a single basic ORC and dual independent basic ORCs. Their model was applied to the geothermal ORC case study from Elsidio et al. (2020).

In the design of geothermal ORC systems, both the configuration and operating conditions (e.g. working fluid temperatures and flowrate) of the ORC are to be optimised. However, in the work of Elsidio et al. (2017), the ORC pressures and temperatures are fixed and not optimised, whilst in the works of Tien et al. (2020) and Dong et al. (2020), only the basic ORC is considered without exploring alternative ORC configurations for improved thermal efficiency. Optimisation without exploring all the degrees of freedom may result in suboptimal solutions. This work addresses the drawbacks of the previous works by enabling simultaneous optimisation of the ORC configuration and operating conditions.

3.1 ORC model

Figure 1a shows a schematic diagram of a modified ORC with regeneration and turbine bleeding for improved thermal efficiency (Desai and Bandyopadhyay, 2009). The working fluid is pressurised through pump 1 (state 1 to 2) and pump 2 (state 3 to 4), evaporated (state 4 to 5), expanded through the turbine (state 5 to 6 and 7) and condensed (state 9 to 1). In the case of a dry fluid, it is assumed that states 1 and 3 are saturated liquid, and that state 5 is saturated vapour. Figure 1b shows the corresponding temperature-entropy diagram. With $t_7 > t_2$, heat exchange between the outlet streams of the turbine and pump 1 (i.e. regeneration) in a regenerator improves the ORC thermal efficiency, which can be further improved by extracting a fraction (x) of the working fluid from the turbine (i.e. turbine bleeding) and mixing it with the outlet stream of pump 1 in a direct contact heater. This increases the inlet temperature of pump 2 (from t_8 to t_3) with reduced work output from the turbine. The direct contact heater and pump 2 are incorporated in the ORC only when there is turbine bleeding; without turbine bleeding, the outlet stream of pump 1 enters the evaporator directly or after regeneration. In addition, the direct contact heater, regenerator, condenser and evaporator are assumed to operate isobarically. The work required for pump 1 ($w_{\text{pump-1}}$) is calculated using Eq(1).

$$w_{\text{pump-1}} = m(1-x)(h_2 - h_1) \quad (1)$$

where h_1 is a function of t^{cond} ; h_2 is a function of t^{cond} and the intermediate temperature (t^{int}); x is the fraction of the working fluid extracted from the turbine. Eq(2) ensures that x lies between the specified lower (X^L) and upper limits (X^U) when there is turbine bleeding ($y = 1$), and forces x to zero when there is no turbine bleeding ($y = 0$).

$$X^L y \leq x \leq X^U y \quad (2)$$

The work required for pump 2 ($w_{\text{pump-2}}$) is calculated using Eq(3).

$$w_{\text{pump-2}} = m(h_4 - h_3) \quad (3)$$

where h_3 is a function of t^{int} , and h_4 is a function of t^{int} and t^{evap} , if $y = 1$, as given in Eqs(4) and (5).

$$H(y-1) \leq h_3 - H_3(t^{\text{int}}) \leq H(1-y) \quad (4)$$

$$H(y-1) \leq h_4 - H_4(t^{\text{int}}, t^{\text{evap}}) \leq H(1-y) \quad (5)$$

The work produced by the turbine (w_{turb}) is calculated using Eq(6).

$$w_{\text{turb}} = mx(h_5 - h_6) + m(1-x)(h_5 - h_7) \quad (6)$$

where h_5 is a function of t^{evap} ; h_6 is a function of t^{evap} and t^{int} ; h_7 is a function of t^{evap} and t^{cond} .

Eq(7) describes the energy balance for the direct contact heater, which acts as a mixer. Eq(8) describes the energy balance for the regenerator. Eq(9) sets an upper limit (Q^U) on the regenerator heat load (q^{reg}), and forces q^{reg} to zero when there is no regeneration ($z^{\text{reg}} = 0$).

$$xh_6 + (1-x)h_8 = h_3 \quad (7)$$

$$q^{\text{reg}} = m(1-x)(h_7 - h_9) = m(1-x)(h_8 - h_2) \quad (8)$$

$$q^{\text{reg}} \leq Q^U z^{\text{reg}} \quad (9)$$

where h_8 is a function of t^{int} and t_8 , and h_9 is a function of t^{cond} and t_9 , if there is regeneration ($z^{\text{reg}} = 1$), as given in Eqs(10) and (11).

$$H(z^{\text{reg}} - 1) \leq h_8 - H_8(t^{\text{int}}, t_8) \leq H(1 - z^{\text{reg}}) \quad (10)$$

$$H(z^{\text{reg}} - 1) \leq h_9 - H_9(t^{\text{cond}}, t_9) \leq H(1 - z^{\text{reg}}) \quad (11)$$

Eqs(12) and (13) ensure feasible heat transfer driving forces if $z^{\text{reg}} = 1$.

$$\Delta T^{\text{min}} - \Gamma(1 - z^{\text{reg}}) \leq t_7 - t_8 \quad (12)$$

$$\Delta T^{\text{min}} - \Gamma(1 - z^{\text{reg}}) \leq t_9 - t_2 \quad (13)$$

where t_2 is a function of t^{cond} and t^{int} ; t_7 is a function of t^{evap} and t^{cond} . In addition, t_4 is a function of t^{int} and t^{evap} if $y = 1$, as given in Eq(14).

$$\Gamma(y - 1) \leq t_4 - T_4(t^{\text{int}}, t^{\text{evap}}) \leq \Gamma(1 - y) \quad (14)$$

The ORC representation in Figure 1a considers four alternative configurations. The modified ORC is simplified to a regenerative ORC when $x = 0$ and $q^{\text{reg}} \neq 0$, to an ORC with turbine bleeding when $q^{\text{reg}} = 0$ and $x \neq 0$, or to a basic ORC when $q^{\text{reg}} = 0$ and $x = 0$. If $y = 1$ ($X^L \leq x \leq X^U$), $t_3 = t^{\text{int}}$ as shown in Figure 1b. If $y = 0$ ($x = 0$), the direct contact heater and pump 2 in Figure 1a will not be incorporated, in which case $h_4 = h_3 = h_8$ and $t_4 = t_3 = t_8$. On the other hand, if $z^{\text{reg}} = 0$ ($q^{\text{reg}} = 0$), then $t_9 = t_7$ and $t_8 = t_2$. All these assignments are ensured by additional enthalpy and temperature constraints, which are omitted due to space limitations.

Eqs(15) and (16) set lower and upper limits on t^{cond} and t^{evap} .

$$T^{\text{cond.L}} \leq t^{\text{cond}} \leq T^{\text{cond.U}} \quad (15)$$

$$T^{\text{evap.L}} \leq t^{\text{evap}} \leq T^{\text{evap.U}} \quad (16)$$

Eq(17) sets lower and upper limits on t^{int} when $y = 1$, while Eq(18) dictates that $t^{\text{int}} = t^{\text{evap}}$ when $y = 0$. This temperature assignment indicates that the outlet pressure of pump 1 will be equal to the vapour pressure of the working fluid at t^{evap} .

$$T^{\text{int.L}} - \Gamma(1 - y) \leq t^{\text{int}} \leq T^{\text{int.U}} + \Gamma(1 - y) \quad (17)$$

$$0 \leq t^{\text{evap}} - t^{\text{int}} \leq \Gamma y \quad (18)$$

Expressions for enthalpies and temperatures at the state points (as functions of temperature) can be obtained from regression analysis within the specified ranges of t^{cond} , t^{int} and t^{evap} . In this work, the thermodynamic properties of the working fluid were calculated using REFPROP, and regressions were performed in Microsoft Excel. All the expressions are linear and have R^2 values greater than 0.99.

3.2 HEN model

Figure 2 shows a stage-wise superstructure for a HEN of process-ORC integration (Lee et al., 2021). The working fluid for the ORC acts as a cold stream when being evaporated (by heat recovery from hot process streams), and as a hot stream when being condensed (by heat exchange with cold process/utility streams). This superstructure does not consider heat exchange between hot ($i \in \mathbf{I}^{\text{ORC}}$) and cold ORC streams ($j \in \mathbf{J}^{\text{ORC}}$), because such heat exchange (i.e. regeneration) has already been considered in the ORC model.

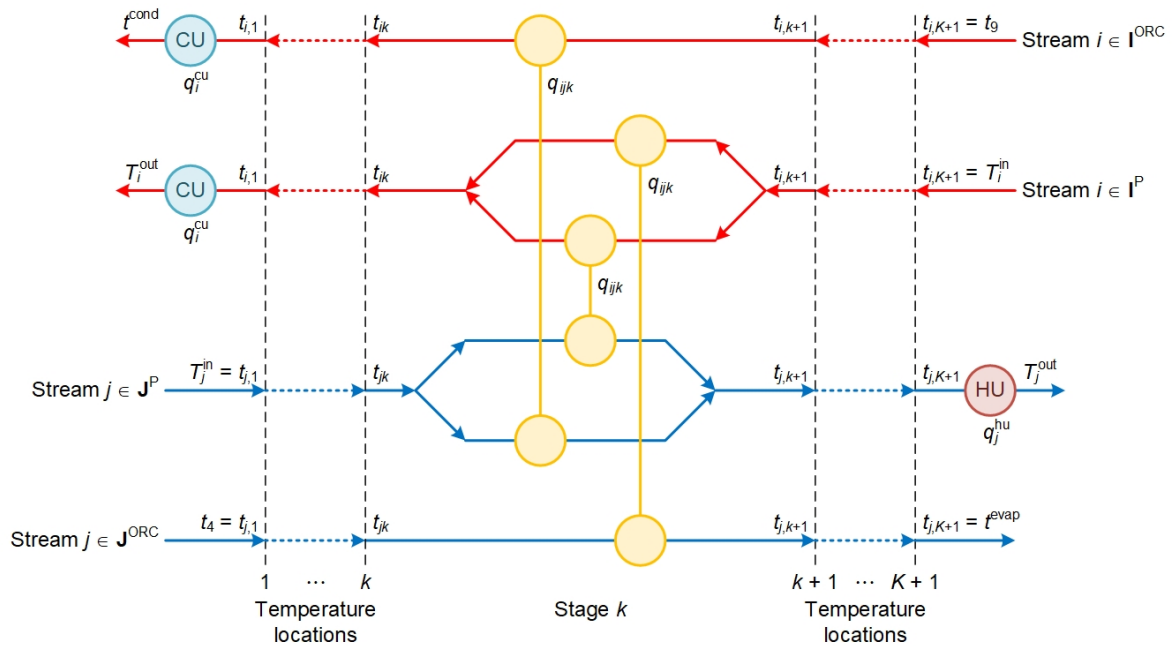


Figure 2: Stage-wise superstructure for an ORC-integrated HEN

In the case of a geothermal ORC system, there is no cold process streams ($j \in \mathbf{J}^P$), and the only hot process stream ($i \in \mathbf{I}^P$) is the geothermal fluid. The corresponding HEN model is a simplified version of the full model presented by Supaluck et al. (2022) by deactivating the constraints and terms for cold process streams. The simplified HEN model consists of constraints for heat balances, temperature assignment and feasibility, feasible latent heat exchange, upper limits on heat loads, and feasible temperature driving forces. Due to space limitations, these constraints are omitted.

3.3 Objective function

To exploit geothermal energy, the objective may be to maximise the net power output of the ORC (f_{WP}), as given in Eq(19).

$$\min f_{WP} = w_{\text{turb}} - (w_{\text{pump-1}} + w_{\text{pump-2}}) \quad (19)$$

With nonlinear terms (arising in energy balance equations) and binary variables in the HEN model, the overall model is a mixed integer nonlinear programme (MINLP). In the next section, a case study is used to illustrate the application of the proposed MINLP model, which is solved in GAMS utilising solver BARON. Solutions were found with negligible processing time (< 2 CPU s).

4. Case study

Table 1 shows the pertinent data for designing a geothermal ORC system using n-pentane (a dry fluid) as the working fluid. This case study, featuring a single hot “process” stream, was originally presented by Elsidio et al. (2017) and then solved by Dong et al. (2020). A minimum temperature difference of 5 °C is assumed for all heat exchange matches (Dong et al., 2020). The condensation temperature of n-pentane is allowed to vary between 20 and 40 °C, the evaporation temperature between 80 and 120 °C, and the intermediate temperature between 50 and 90 °C (if there is turbine bleeding). These temperature limits are based on considerations including the geothermal fluid temperature, the normal boiling point and critical temperature of the working fluid, and the cold utility temperature. For results comparison, the condensation temperature for the ORC is set to 25 °C as in the work of Dong et al. (2020). In addition, isentropic efficiencies of the pump and turbine are assumed to be 70 and 82 % (Elsidio et al., 2017).

Table 1: Stream data for the case study

Stream	Heat capacity flowrate (kW/K)	Supply/inlet temperature (°C)	Target/outlet temperature (°C)
H1 (geothermal fluid)	125	150	70
CU (cooling water)	To be determined	15	20

Solving the ORC-HEN model yields the optimal design in Figure 3a. The maximum net power output is found to be 1,275.07 kW, which can be achieved using a regenerative ORC with three heat exchange units (one exchanger, one cooler and a regenerator). The optimal evaporation temperature and flowrate of n-pentane are determined to be 87.09 °C and 23.28 kg/s. Compared to the results of Dong et al. (2020) using a single basic ORC – 20.99 kg/s of n-pentane evaporated at 93.3 °C and condensed at 25 °C with a net power output of 1,254.1 kW, the proposed model provides a better solution with a higher net power output and fewer heat exchange units (three versus four). It is also worth noting that the results of Dong et al. (2020) violates the overall energy balance. Specifically, the energy output (1,254.1 kW of net power output + 8,803.8 kW of heat rejected to the cold utility = 10,057.9) of the ORC is greater than the energy input (10,000 kW of heat absorbed from H1). Such discrepancies are avoided in this work.

The condensation temperature for the ORC (25 °C) is lower than the normal boiling point of n-pentane (36 °C). In other words, the condensation pressure of n-pentane at 25 °C is lower than the atmospheric pressure. In that case, the ambient air will leak into the system, reducing the thermal efficiency and leading to poor heat transfer performance in the evaporator (Desai and Bandyopadhyay, 2009). To avoid such operational issues, the above ambient condensation pressure criterion should be satisfied. Solving the ORC-HEN model with t^{cond} no lower than 36 °C yields the optimal design in Figure 3b. The maximum net power output is found to be 1,010.59 kW, which can be achieved using a regenerative ORC with three heat exchange units (one exchanger, one cooler and a regenerator). However, since not all the heat available from H1 is transferred to the working fluid in the evaporator (with 565.87 kW left), another cooler is needed for H1 to achieve its target temperature. The optimal condensation temperature, evaporation temperature and flowrate of n-pentane are determined to be 36 °C, 92.9 °C and 21.41 kg/s. Despite a reduced net power output, the design in Figure 3b is more practical avoiding leakage of ambient air in the system.

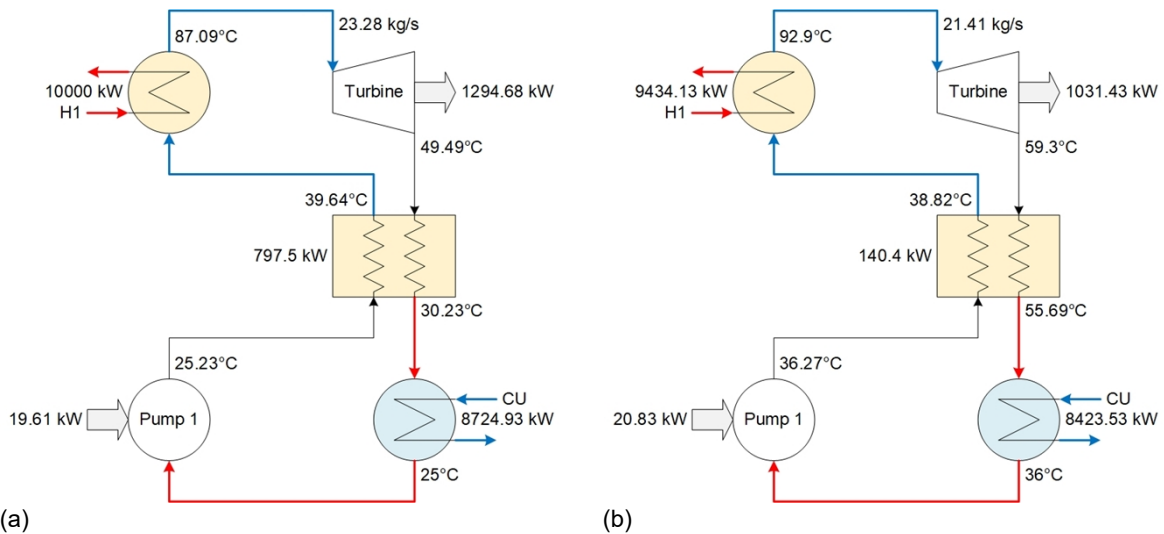


Figure 3: Optimal ORC designs for $t^{cond} = 25\text{ °C}$ (a) and $t^{cond} = 36\text{ °C}$ (b)

5. Conclusions

A simultaneous optimisation approach to the synthesis of ORC-integrated HENs has been developed in this paper. The mathematical model considers four alternative ORC configurations (basic; with regeneration, turbine bleeding or both), and treats the flowrate, operating temperatures and enthalpies of the ORC working fluid as variables. The thermodynamic properties (e.g. enthalpies and pump/turbine outlet temperatures) of the ORC working fluid are correlated as functions of its operating temperatures through regression analysis. A literature case study was solved to demonstrate the application of the proposed model. The resulting geothermal ORC design achieves a slightly higher thermal efficiency with fewer heat exchangers when compared with the results of Dong et al. (2020) using a single basic ORC. Future work will consider dual ORCs with multiple evaporation/condensation temperature levels and alternative working fluids, as well as the trade-off between energy and capital costs with the objective of minimising the total annualised cost. The simultaneous optimisation approach can be extended to the design of solar thermal ORC systems.

Nomenclature

H – arbitrary large value, kJ/kg

Γ – arbitrary large value, °C

h_* – specific enthalpy at state point $*$, kJ/kg

t_* – temperature at state point $*$, °C

y – 0 or 1, whether or not there is turbine bleeding

z^{reg} – 0 or 1, whether or not there is regeneration

Acknowledgments

This research was funded by the Ministry of Science and Technology, Taiwan, R.O.C. (Project No. 109-2221-E-027-038). The authors thank the “Research Center of Energy Conservation for New Generation of Residential, Commercial, and Industrial Sectors” for financial support from the Featured Areas Research Center Program within the framework of the Higher Education Sprout Project by the Ministry of Education, Taiwan, R.O.C.

References

- Desai N.B., Bandyopadhyay S., 2009, Process integration of organic Rankine cycle, *Energy*, 34, 1674–1686.
- Dong X., Liao Z., Sun J., Huang Z., Jiang B., Wang J., Yang Y., 2020, Simultaneous optimization of a heat exchanger network and operating conditions of organic Rankine cycle, *Industrial & Engineering Chemistry Research*, 59, 11596–11609.
- Elsido C., Mian A., Martelli E., 2017, A systematic methodology for the techno-economic optimization of Organic Rankine Cycles, *Energy Procedia*, 129, 26–33.
- IEA, 2021, Net Zero by 2050, International Energy Agency, Paris <<https://www.iea.org/reports/net-zero-by-2050>> accessed 13.05.2022.
- Lee J.-Y., Watanapanich S., Li S.-T., 2021, Optimal integration of organic Rankine cycles into process heat exchanger networks, *Chemical Engineering Transactions*, 88, 571–576.
- Watanapanich S., Li S.-T., Lee J.-Y., 2022, Optimal integration of organic Rankine cycles into process heat exchanger networks: A simultaneous approach, *Energy Conversion and Management*, 260, 115604.